Stabilization of PFAS-contaminated soil with activated biochar

Erlend Sørmo [a,b,*], Ludovica Silvani [a], Nora Bjerkli [b], Nikolas Hagemann [c,d], Andrew R. Zimmerman [f], Sarah E. Hale [a], Caroline B. Hansen [a], Thomas Hartnik [e], Gerard Cornelissen [a,b]

[a] Department of Environmental Chemistry, Norwegian Geotechnical Institute (NGI), Oslo, Norway
[b] Faculty of Environmental Science and Natural Resource Management (MINA), University of Life Sciences (NMBU), Ås, Norway
[c] Agroscope, Reckenholz, Switzerland
[d] Ithaka Institute for Carbon Strategies, Arbaz, Switzerland and Freiburg, Germany
[e] Lindum AS, Drammen, Norway
[f] Department of Geological Sciences, University of Florida, Gainesville, FL, USA

HIGHLIGHTS

- Waste timber biochars reduce leaching of polyfluoroalkyl substances from soil.
- Sorbent effect is proportional to degree of activation and activation temperature.
- Effects of steam and carbon dioxide activation agents are similar.
- Soil organic carbon content influences sorbent effectiveness.
- Biochar sorbents can be tailored to remediation requirements through activation.

GRAPHICAL ABSTRACT
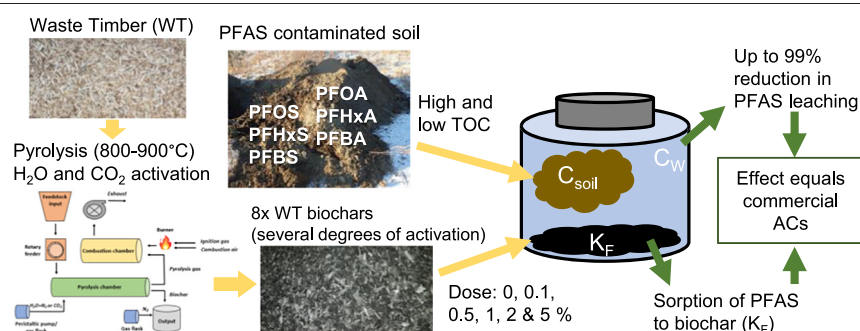
ABSTRACT

Biochars are considered potential sustainable sorbents to reduce the leaching of *per-* and polyfluoroalkyl substances (PFAS) from contaminated soils. However, biochar characteristics must probably be optimized to achieve useful sorption capacity. In the present work, eight waste timber biochars were produced, including biochars activated to different degrees, at different temperatures, and using both steam and CO_2. In laboratory batch experiments, the eight biochars were amended to soil samples from two different horizons, with low and high total organic carbon (TOC, 1.6% and 34.2%, respectively), of a heavily PFAS-contaminated soil (1200–3800 µg kg^{-1} PFAS$_{tot}$), at varying doses (0, 0.1, 0.5, 1.0 and 5.0%). With a 5% amendment to the low-TOC soil, all eight biochars resulted in strongly reduced leachate PFAS concentrations (by 98–100%). At the same amendment dose in the high-TOC soil, leachate concentration reductions were more modest (23–100%). This was likely due to a strong PFAS-sorption to the high-TOC soil itself, as well as biochar pore clogging in the presence of abundant organic matter, resulting in fewer sorption sites available to PFAS. Reduction in PFAS leaching was proportional to the degree of activation and activation temperature. Thus, lower amendment doses of activated biochars were needed to reduce PFAS leaching to the same level as with the non-activated biochar. Activation however, came at a tradeoff with biochar yield. Furthermore, the adsorption ability of these biochars increased proportionally with PFAS-fluorocarbon chain length, demonstrating the role of hydrophobic interactions in reduction of PFAS leaching. Development of internal surface area and porosity was proposed as the main factor causing the improved performance of activated biochars. This study shows that woody residues such as waste timber can be used to produce effective sorbents for the remediation of PFAS-contaminated soil. It also highlights the desirability of sorbate and matrix-specific optimization of biochar production.

© 2020 The Author(s). Published by Elsevier B.V. This is an open access article under the CC BY license (http://creativecommons.org/licenses/by/4.0/).

* Corresponding author at: Department of Environmental Chemistry, Norwegian Geotechnical Institute (NGI), Oslo, Norway.
E-mail address: ers@ngi.no (E. Sørmo).

1. Introduction

Per- and polyfluoroalkyl substances (PFAS) are found in soils all over the world (Rankin et al., 2016). This is a direct result of five decades of widespread production, use, and subsequent release of PFAS from local point sources such as fluorochemical plants (Jin et al., 2015), firefighting training facilities (Banzhaf et al., 2017), metal and paper industry (Clara et al., 2008), landfills (Lang et al., 2017), and waste water treatment plants, which usually fail to effectively eliminate PFAS (Gallen et al., 2018). Additionally, there are diffuse sources, such as biosolids used for agricultural purposes (Gallen et al., 2018; Sepulvado et al., 2011) and long range atmospheric transport to rural areas (Chen et al., 2016) and the remote Arctic (AMAP, 2016; Skaar et al., 2019).

The physiochemical properties of PFAS have been linked to persistency in the environment, toxicity and bioaccumulation in food chains (Krafft and Riess, 2015; Lau et al., 2007; Sunderland et al., 2019). Furthermore, various PFAS readily leach from soils to groundwater and surface water (Banzhaf et al., 2017). This leachability is illustrated by low partitioning coefficients between soil organic carbon (OC) and water (K_{OC}) reported for perfluorooctanesulfonic acid (PFOS, $10^{3.0\pm0.7}$ L kg^{-1}) and perfluorooctanoic acid (PFOA, $10^{2.1\pm1.0}$ L kg^{-1}) in soils and sediments (Zareitalabad et al., 2013), compared to the higher K_{OC} of strongly sorbing compounds such as polycyclic aromatic hydrocarbons (PAHs), e.g. phenanthrene ($10^{4.37\pm0.17}$ L kg^{-1}) or pyrene ($10^{5.11\pm0.15}$ L kg^{-1}) (Chiou et al., 1998). The problematic properties and ubiquitous presence of PFAS in soils has prompted a need for effective remediation techniques (Mahinroosta and Senevirathna, 2020).

To reduce the leaching of contaminants, sorbent amendments have been explored for the last couple of decades for use in both sediment (Cornelissen et al., 2012; Ghosh et al., 2011) and soil remediation (Beesley et al., 2011; Rajapaksha et al., 2016). Carbon-based sorbents can bind organic contaminants strongly, reducing their leachable and bioavailable fractions (Hale et al., 2012; Zhang et al., 2013), and thus, their environmental impact and health risks (Ehlers and Luthy, 2003). Recent studies have shown that both commercially available activated carbon (AC) and biochar can be used to reduce the mobility of PFAS in soils (Askeland et al., 2020; Hale et al., 2017; Kupryianchyk et al., 2016b; Silvani et al., 2019; Sorengard et al., 2019; Sörengård et al., 2019). In a recent review of remediation alternatives for PFAS-contaminated soils (Mahinroosta and Senevirathna, 2020), it was concluded that immobilization with carbonaceous sorbents is among the most promising options.

Biochar, the carbonaceous product of biomass pyrolysis, can be produced from a wide range of feedstocks under variable pyrolysis conditions, resulting in a material with a variety of physiochemical properties that can be optimized for specific applications (Lehmann and Joseph, 2015). To strongly bind organic contaminants, a large specific surface area (SSA) is desirable (Ahmad et al., 2014; Beesley et al., 2011; Hale et al., 2016; Zhang et al., 2013). A pyrolysis temperature of more than 600 °C is commonly needed to achieve significant porosity, rendering a large internal SSA where strong adsorption of aromatic organic compounds, such as PFAS, can take place (Zhao et al., 2013). The greater sorption affinities of higher temperature chars for organic contaminants are mainly explained by their high degree of aromatic condensation (Keiluweit et al., 2010).

Activation can improve the sorptive ability of biochar by expanding its surface area through the creation of new nanopores (<2 nm), as well as by creating 'clean' aromatic surfaces free of non-aromatic moieties and functional groups (Baharak et al., 2019; Marsh and Reinoso, 2006). These pores can be created through either physical or chemical activation processes. In physical activation, carbon on the biochar surface is oxidized by steam (H_2O) or carbon dioxide (CO_2), preferably at temperatures above 850 °C, while new pore spaces are created by oxidizing secondary char that was formed as condensates during pyrolysis (Hagemann et al., 2018). In chemical activation, biochar is mixed with dewatering and/or oxidizing agents, e.g. $ZnCl_2$, H_2PO_4 or KOH (Martin

et al., 1996), with the advantage that it can be done at a lower temperature (500 °C) compared to physical activation (>850 °C) (Hagemann et al., 2018), and disadvantages of the use of corrosive chemicals and environmentally harmful pollutants, and the necessity to remove the activation agent (Marsh and Reinoso, 2006). Therefore, the present study focused on physical activation.

The conditions of physical activation should be optimized for the intended application. Hagemann et al. (2020) used physical activation of woody residues to produce sorbents with properties comparable to commercially available activated carbon (AC) in removing micropollutants from wastewater. They showed that the dose of the activation agent (H_2O/CO_2), i.e. the degree of activation, had pronounced impacts on sorption properties. To date, no study has quantified the effect of degree of activation, activation temperature and activation agent type on PFAS sorption to biochar in soil.

Attention has been drawn to the potential benefits of producing sorbents by pyrolysis and/or activation of waste fractions other than agricultural residuals, such as sewage sludge (Agrafioti et al., 2013), impregnated waste timber (Helsen and Van den Bulck, 2000; Zhurinsh et al., 2005), paper mill effluent (Devi and Saroha, 2014), food waste (Grycová et al., 2016), scrap tires (Chen et al., 2007) and waste mixtures (Bernardo et al., 2012). These sorbents could potentially be sustainable alternatives to traditional AC made from fossil hard coal (Benedetti et al., 2017), improving the overall environmental benefits of remediation projects in a life cycle perspective (Alhashimi and Aktas, 2017; Sparrevik et al., 2011).

Pyrolysis emissions and the quality of biochar produced from non-impregnated waste timber (WT), as well as the possible use of such biochar for soil remediation purposes, has been explored in two recent studies (Silvani et al., 2019; Sørmo et al., 2020). Waste timber, a common waste fraction handled by Norwegian recycling companies (750,000 t y^{-1} SSB (2018)), is a mixture of discarded wood from industry, demolition and wood waste collected at municipal recycling stations. Chemically impregnated wood waste is not included in this fraction.

In the present study, the ability of non-activated and activated WT biochar, produced under 8 different conditions, to reduce the leaching of PFAS from field-contaminated soils was investigated. The overarching goal of the study was to examine the potential of WT biochar to stabilize PFAS-contaminated soil and whether the process of physical activation can be adjusted as to optimize biochar sorbents to meet challenging site-specific remediation benchmarks. Studying a suite of activated biochars and PFAS in two distinctly different soil samples allowed for novel mechanistic understanding of the processes governing the binding of PFAS to biochar amendments in the presence of soil.

2. Materials and methods

2.1. Soils

The soil used in this study was a contaminated podzolized moraine soil from a former firefighting training facility at Rygge Airport, Norway (59.3732 N, 10.7935 E). This area, located in the South-Eastern part of Norway, receives snow in the winter, is fully humid and has warm summers; classified as Dfb according to the Köppen climate classification (Kottek et al., 2006). Being situated close to the post-glacial marine divide, the local quaternary deposits are marine shoreline sediments (≥0.5 m) dominated by sand and gravel (NGUa, n.d.-a), above bedrock consisting of granitic gneiss (NGUb, n.d.-b).

Two large bulk samples (~140 L each) were collected by a waste handling company (Lindum AS) through randomized multiple grab sampling from: 1) the upper organic horizon (high-TOC soil), and 2) the underlying eluvial and illuvial mineral horizons (low-TOC soil). A subsample (~20 L) obtained from each of these bulk samples was homogenized thoroughly by mixing in plastic tubs and roots, twigs and

rocks (>2 cm) were removed by sieving before they were stored in polyurethane bags in the dark at 4 °C prior to analysis.

TOC-content was determined according to ISO 10694, and pH by potentiometry in a 0.01 M $CaCl_2$ solution according to standard DIN ISO 10390 by the accredited laboratory Eurofins Norway (Eurofins).

PFAS content in each soil (22 compounds, se supporting information (SI) S.2 for complete list) was determined by Eurofins according to method DIN 38414-S14, using a methanol or acetonitrile ultrasonic extraction with a multiple step solvent clean up, solid phase extraction, and quantification by liquid chromatography coupled with tandem mass spectrometry (LC/MS-MS). Limits of quantification for the PFAS analysed are given in the SI (Table S11). Uncertainty related to heterogeneity of PFAS concentrations in the soil samples and potential sampling bias was estimated using the relative standard deviation of triplicate analyses (provided in Table S8).

The soil samples were also screened in triplicates for aliphatic compounds (C5-C35) using GC–MS according to SPI 2011 and polycyclic aromatic hydrocarbons (PAHs) using GC–MS according to ISO 18287 by Eurofins Norway.

2.2. Biochar sorbents

2.2.1. Feedstock

As reported previously, Sørmo et al. (2020) collected and shredded (10 mm) three random batch samples of waste timber (WT 1–3, ~500 kg each) from a waste handling company (Lindum AS, Drammen, Norway). A WT sample (27 L) was obtained for the present study by mixing three randomized samples (3 L) from each of the previously collected large bulk samples (WT 1–3). The WT subsample was crushed further with a cutting mill and sieved to obtain a 2–4 mm particle size fraction for pyrolysis.

2.2.2. Pyrolysis and activation

Both pristine and activated WT biochar was produced using an experimental pyrolysis unit PYREKA (Pyreg, Dörth, Germany) with a 1 m long electrically heated and continuously fed auger system (Fig. S1, Hagemann et al. (2020)). Residence time in the pyrolysis chamber was 12 min, and each batch of biochar was produced for at least 36 min (=three reactor volumes). Activation and pyrolysis were performed as a one-step process (Hagemann et al., 2020), i.e. the feedstock was directly exposed to the conditions of activation. Each batch was separated by producing and discarding the biochar of three reactor volumes after changing the conditions.

Eight biochars were produced with different activation conditions (varying activation temperature, agent and dose) (Table 1). These included non-activated biochar produced at 900 °C (BC900), activated biochar produced at 900 °C with molar ratios of H_2O to feedstock carbon of 0.50, 0.75, 1.00 and 1.25 (aBC900-0.5, aBC900-0.75, aBC900-1.00 and aBC900-1.25, respectively), biochar activated with steam at molar ratio

of H_2O to feedstock carbon of 1 at 850 and 800 °C (aBC850-1.00 and aBC800-1.00, respectively) and biochar activated at 900 °C with CO_2 at a molar ratio of CO_2 to feedstock carbon of 1 (aBC900-1.00 CO_2).

To produce non-activated biochar, the reactor was flushed with 2 L min^{-1} N_2. For steam activation, water was injected with a peristaltic pump into the stream of N_2. In the reactor, it is assumed the water undergoes an immediate phase change, as the critical temperature of water is 374 °C. For CO_2 activation, this gas was used instead of water. In practice, oxidation does not happen at a 1:1 ratio between oxidant and feedstock C, hence a ratio of 1.25 will still render a significant biochar yield (8%, Table 1) without the full oxidation of the biochar matrix. Exact amounts of activation agents were calculated on the basis of feedstock carbon content and feedstock feed rate. Biochar yield was calculated as the quotient of biochar production rate (g min^{-1}) and WT feed rate (g min^{-1}).

2.2.3. Biochar properties

Specific surface area (SSA) and pore volume were determined by N_2 gas adsorption and BET data evaluation for pores >1.5 nm and by CO_2 gas adsorption for pores 0.4–1.5 nm, according to the theory described by Kwon and Pignatello (2005), on a Quantachrome Autosorb I (at the Particle Engineering Research Center, University of Florida). Elemental content (C, N and H) was quantified with a Leco CHN-1000 from Leco Corporations, Sollentuna, Sweden, according to DIN 51732.

2.3. PFAS leaching tests

The leachable PFAS was determined using a one-step aqueous batch shaking test with a liquid to solid mass ratio (L/S) of 10, in accordance with CEN EN 12457 with modification (Hale et al., 2017; Kupryianchyk et al., 2016b). The batch shaking test is a rigorous procedure that simulates a worst-case scenario where contaminated soil is flushed with large amounts of water.

Soil or soil/biochar (40 g dry matter) and water (400 mL, 18 MΩ) were placed into pre-cleaned (methanol, 10%) polyethylene bottles (500 mL). The soil/biochar was pre-mixed by adding different amounts of biochar (0%, 0.1%, 0.5%, 1%, 2%, and 5% of d.w.) to soil (40 g d.w.). Before mixing, the soils were dried at 105 °C for 24 h and both soil and biochar were crushed and sieved to particles of <1 mm. The bottles were agitated on a shaking table (100 rpm) at room temperature (20 °C) for 14 days and were then left to settle for 2 days (at 4 °C) before filtration through a 1.2 μm glass microfiber filter (Whatman, grade GF/C). A subsample for dissolved organic carbon (DOC) analysis was filtered using 0.45 μm polyethersulfone membrane and the filtrate was analysed by infrared spectrometry according to method NS-EN 1484 by Eurofins. The pH in the filtrates were measured by potentiometry according to ISO 10523 Eurofins.

All 22 PFAS were determined in the filtrate as described for soil, i.e. using LC/MS-MS according to method DIN 38414-S14, by the accredited

Table 1
Activation agent molar ratio of activation agent to feedstock carbon (−), activation temperature (°C), mass and carbon yield (%), surface area (m^2 g^{-1}), pore volume (%) and elemental content (C, O, N, %) and ratios for the biochars produced for the leaching tests.

#	Biochar sorbent	Activation agent	Molar ratio of activation agent to feedstock C	Activation temperature (°C)	Biochar weight yield (%)	Biochar C-yield (%)	N$_2$ sorption (pores > 1.5 nm)		CO$_2$ sorption (pores 0.3–1.5 nm)		Elemental content			Elemental ratio	
							Surface area (m^2 g^{-1})	Pore volume (%)	Surface area (m^2 g^{-1})	Pore volume (%)	C (%)	O (%)	N (%)	C/O	C/N
1	BC900	None (N$_2$)	0	900	19.0	34.9	411	28	840	24	88.8	6.82	1.01	13	88
2	aBC900-0.50	Steam (H$_2$O)	0.50	900	12.2	22.3	550	45	744	22	90.6	5.87	0.84	15	107
3	aBC900-0.75	Steam (H$_2$O)	0.75	900	12.1	22.2	605	52	746	23	89.0	5.58	0.78	16	114
4	aBC900-1.00	Steam (H$_2$O)	1.00	900	8.9	16.3	713	83	750	24	87.7	7.98	0.75	11	117
5	aBC900-1.25	Steam (H$_2$O)	1.25	900	8.0	14.7	623	51	846	28	86.9	5.67	0.78	15	112
6	aBC800-1.00	Steam (H$_2$O)	1.00	800	16.3	29.9	444	32	620	20	89.4	5.41	0.93	16	96
7	aBC850-1.00	Steam (H$_2$O)	1.00	850	12.6	23.2	740	86	805	24	89.2	5.84	0.86	15	103
8	aBC900-1.00-CO$_2$	CO$_2$	1.00	900	12.5	23.0	617	43	850	26	89.5	5.38	1.16	17	77

laboratory Eurofins Norway. Limits of quantification for the PFAS analysed are given in the SI (Table S11).

In order to obtain a measure of the uncertainty of the method used, eight of the total 82 tests (2 soils × 5 doses × 8 biochars + 2 soil controls) were repeated in triplicates: two biochar types (BC900 and aBC900-1.00) at two different doses in both soils (0.5% and 2% for High-TOC soil and 0.1% and 1% for Low-TOC soil). To express the uncertainty in PFAS leaching for the non-replicated tests, the third quartile value for the observed relative standard deviations in the eight triplicate tests were used for each measured PFAS. This approach provided a conservative estimation of uncertainty as it ensured the expressed uncertainty for each leachate concentration would be equal to or lower than that observed in 75% of the cases. More details are proved in section S.1.3 of the SI.

2.4. Data analysis

The effect of the biochar amendment on leaching was expressed as the percentage reduction in leaching ($F_{reduced}$) from an amended soil ($C_{w,amended}$) relative to the unamended soil ($C_{w,control}$):

$$F_{reduced}(\%) = \left(1 - \left[C_{w,amended}\left(\mu g\ L^{-1}\right)/C_{w,control}\left(\mu g\ L^{-1}\right)\right]\right) \times 100 \quad (1)$$

The partitioning coefficients (K_D) for PFAS between soil (C_{soil}) and leachate water (C_w) in the unamended soil samples were calculated assuming a linear sorption model:

$$K_D\left(L\ kg^{-1}\right) = C_{soil}\left(\mu g\ kg^{-1}\right)/C_w\left(\mu g\ L^{-1}\right) \quad (2)$$

Here C_{soil} at equilibrium was calculated by subtracting the leachable concentration from the initial soil concentration (see S.1.2 in the SI for more details).

As the sorption to biochar is non-linear (Hale et al., 2016; Kupryianchyk et al., 2016a), biochar-water distribution should be described by the non-linear Freundlich isotherm sorption model (Schwarzenbach et al., 2003):

$$K_F\left(L\ kg^{-1}\right) = C_w^n\left(\mu g\ L^{-1}\right)/C_{biochar}\left(\mu g\ kg^{-1}\right) \quad (3)$$

K_F can be determined in the presence of soil by using a mass balance approach for the whole system of soil, water and biochar as described by Silvani et al. (2019). A more detailed description of the approach can be found in the SI (S.1.2).

If an isotherm cannot be properly constructed, K_F-values can be calculated for C_W interpolated to 1 µg L^{-1} or 1 ng L^{-1} by using a Freundlich nonlinearity coefficient, $n = 0.7$, obtained previously (Cornelissen et al., 2005). Thus, a concentration dependent K_D value for the partitioning between biochar and water should be derived through the non-linear Freundlich model.

Single linear regression analyses and *t*-tests were carried out using 'R' software (v.3.4.3). Data was tested for normality using the Shapiro-Wilk test. Normally distributed data was compared using a Welch two-sample t-test, while non-normally distributed data was compared using the Mann-Whitney-Wilcoxon test. Results were considered statistically significant for *p* < 0.05.

3. Results and discussion

3.1. Soil properties

The high-TOC soil from the O-horizon had a TOC content of 34.2% with a pH of 4.9, while the low-TOC soil from the eluvial and illuvial horizons had a TOC content of 1.6% and a pH of 7.8.

Of the 22 PFAS screened, 14 were detected in both soil samples (PFBS, PFHxS, PFHpS, PFOS, PFDS, PFBA, PFDS, PFBA, PFPeA, PFHxA, PFHpA, PFOA, PFNA, PFOSA, 6:2 FTS and 8:2 FTS), while PFDeA was only detected in the low-TOC soil (Table S1 in the SI). The sum of detected PFAS (PFAS_tot), was about three times higher in the low-TOC soil (3800 ± 240 µg kg^{-1} d.w.) than the high-TOC soil (1200 ± 80 µg kg^{-1} d.w.). The distribution of PFAS was similar in both samples with the two perfluorinated sulfonic acids (PFSA), PFOS and PFHxS, being the two most abundant compounds, representing >95% of the total PFAS content. PFOS concentrations were 3400 ± 200 µg kg^{-1} (89.5%) and 1000 ± 60 µg kg^{-1} (83.3%), and PFHxS concentrations were 200 ± 18 µg kg^{-1} (5.3%) and 110 ± 24 µg kg^{-1} (9.2%) in low-TOC and high-TOC soils, respectively. The high concentrations of PFOS is a result of the historic use of aqueous film-forming foams (AFFF) at the firefighting training facilities of Rygge Airport. The remainder of detected PFAS in both soils were all <1.5% of the total.

Significant but low PAH contents were detected in the low-TOC soil ($\sum PAH_{16} = 0.33 \pm 0.16$ mg kg^{-1}, Table S2), but no aliphatic compounds were quantified. No PAHs (<0.045 mg kg^{-1}, Table S2), but significant long chain aliphates (C16–C35, 513 ± 6 mg kg^{-1}), were detected in the high-TOC soil. It is not known whether these aliphatic compounds originate from fossil mineral oil contamination or from the natural organic matter of the O-horizon.

3.2. Biochar properties

Properties of the eight biochars are shown in Table 1. The biochar yield decreased significantly with molar ratio of oxidant to feedstock C ($R^2 = 0.94$, $p > 0.05$), from 19% (non-activated) to 8% (most activated). The total carbon content was about 90% for all the biochars produced, and there was no significant correlation between biochar carbon content and degree of activation (0–1.25) or activation temperature (800–900 °C). However, a significant correlation between biochar carbon yield and degree of activation (0–1.25) was observed ($R^2 = 0.97$, $p = 0.007$).

Non-activated biochar produced at 900 °C exhibited an SSA of 840 m² g^{-1} for small pores (0.3–1.5 nm, CO_2 gas adsorption) and 411 m² g^{-1} for larger pores (>1.5 nm, N_2 gas adsorption) (Table 1). As expected, the SSA of this biochar made at this high temperature was larger than that of biochar made from the same feedstock at a lower temperature (500–600 °C) reported in two previous studies, where the SSAs were 450–525 m² g^{-1} (pores 0.3–1.5 nm) and 130–280 m² g^{-1} (pores > 1.5 nm) (Silvani et al., 2019; Sørmo et al., 2020), although different pyrolysis units were used in these studies. The high pore SSA is furthermore similar to SSA for biochar produced from pine saw dust (397 ± 4 m² g^{-1}) at 750 °C (Askeland et al., 2019).

No significant linear relationship was observed between CO_2-SSA of small 0.3–1.5 nm pores and degree of activation (p > 0.05). For the larger >1.5 nm pores however, N_2-SSA increased significantly with degree of activation ($R^2 = 0.78$, $p = 0.047$). However, at the highest molar ratio of oxidant to feedstock C, 1.25, the SSA of larger pores started to decrease again. This is likely the result of pore structure collapse from the interaction with excess oxidant (Hagemann et al., 2018; Hao et al., 2013).

Activation with CO_2 (aBC900-1.00-CO_2) resulted in similar SSA and porosity as activation with steam (aBC900-1.00) but created a different distribution of pore sizes (Table 1). Specific surface area of large pores was ~100 m² g^{-1} higher in the steam activated biochar (713 versus 617 m² g^{-1}) while SSA of small pores was 100 m² g^{-1} smaller in the steam activated biochar (750 versus 850 m² g^{-1}) compared to the CO_2 activated biochar. Activation by CO_2 is expected to create new pore spaces while steam activation expands existing pores (Aworn et al., 2008). This potentially explains why the aBC900-1.00-CO_2 lost less of the small pore SSA (collapse of micropores offset by creation of new ones) but did not produce the same increase in large pore SSA as the aBC900-1.00 (more expansion of existing pores) compared to non-activated BC900.

There were no significant linear correlations between SSA or porosity and activation temperature, but the range of studied temperatures was small (800–900 °C) with few data points ($n = 3$). Specific surface area for small pores and large pores were, however, >200 m^2 g^{-1} and >100 m^2 g^{-1} larger for biochar activated at 900 °C than biochar activated at 800 °C, respectively. This indicates that the higher activation temperature (900 °C) is preferable for creation of a large internal SSA. However, it was not tested for whether elongated residence time could compensate for lower pyrolysis temperature.

3.3. PFAS leached from unamended soil

The leaching of PFAS from the unamended soils was dominated by the two compounds present at the highest concentrations in the soil, PFOS and PFHxS (Table 2). Leachate concentrations of PFOS were 2.9 ± 0.6 µg L^{-1} and 240 ± 50 µg L^{-1} in high-TOC and low-TOC soil, respectively. Corresponding concentrations for PFHxS were 1.2 ± 0.3 µg L^{-1} and 26 ± 5 µg L^{-1}, respectively.

In the low-TOC soil leachate, all 14 PFAS quantified in the soil sample (Table S1) were detected, whereas in the high-TOC soil only 9 of the 13 quantified in the soil were also detected in the leachate (PFBS, PFHxS, PFHpS, PFOS, PFBA, PFPeA, PFHxA, PFHpA and PFOA). It is thus likely that the PFAS present in the high-TOC soil but not in its leachate (PFNA, PFOSA, 6:2 FTS and 8:2 FTS, all with CF-chain ≥6) were strongly retained by organic matter (OM). The sorption of PFAS has been found to increase with OM content in soils (Campos Pereira et al., 2018) and sediments (Higgins and Luthy, 2006). Furthermore, PFAS sorption has been shown to increase linearly with fluorocarbon (CF) chain length (for the CF3–CF9 chain lengths considered here) (Campos Pereira et al., 2018; Sorengard et al., 2019).

The effect of soil OC in reducing PFAS leaching is further exemplified by the lower K_D-values of PFOS in the low-TOC soil ($10^{0.6}$ L kg^{-1}) versus the high-TOC soil ($10^{2.5}$ L kg^{-1}). The importance of OC for sorption to the unamended soils was also illustrated by the similarity of the carbon content-normalized distribution coefficients K_{OC} (calculated as K_D/f_{OC}) for both soils; K_{OC} values were $10^{2.6}$ and $10^{3.0}$ L kg^{-1} for PFOS and $10^{1.9}$ and $10^{2.5}$ L kg^{-1} for PFOA for low-TOC and high-TOC soil, respectively.

Literature partitioning coefficients for PFAS in soil are relatively scarce, but the calculated logK_{OC} values in this study are similar to soil and sediment values reported by Zareitalabad et al. (2013) for PFOS ($10^{2.4}$–$10^{4.7}$ L kg^{-1}) and PFOA ($10^{1.3}$–$10^{4.5}$ L kg^{-1}), but lower than some of the values reported by Kupryianchyk et al. (2016b) for PFOS, PFHxS and PFOA ($10^{1.53}$–$10^{6.00}$ L kg^{-1}).

3.4. Reduction in PFAS leaching from amended soil

In the following discussion, the main focus will be on three PFSA and three perfluorinated carboxylic acids (PFCA) that had a dominating

presence in both soils and their leachates and represent a range in CF-chain lengths: PFBS (CF4), PFHxS (CF6), PFOS (CF8), PFBA (CF3), PFHxA (CF5) and PFOA (CF7). Concentrations of all PFAS analysed in leachates from both unamended and amended soils are presented in the SI (Tables S3 and S4).

3.4.1. Effect of sorbent dose and soil type

Generally, the effect of biochar sorbents on reduction in PFAS leaching ($F_{reduced}$) was strong in the low-TOC soil, but not as pronounced in the high-TOC soil (Fig. 1, Tables S5 and S6). In the low-TOC soil, a high $F_{reduced}$ ($>90\%$) was observed for all sorbents at doses of 0.5% or greater except the non-activated biochar (BC900) (Fig. 1). At a 0.5% dose, activated biochars reduced leaching by $>90\%$ for PFBS, PFHxS, PFOS, PFHxA and PFOA, but somewhat lower for PFBA ($>57\%$). At higher doses (1–5%), the reduction in leaching was $>98\%$ for PFBS, PFHxS, PFOS, PFHxA and PFOA, and $> 79\%$ for PFBA. For the non-activated BC900, a dose of 2% was needed for reduction in PFBS, PFHxS, PFOS, PFHxA and PFOA leaching $> 90\%$, and a dose of 5% for the same reduction PFBA leaching.

The reduction of PFAS-leaching from the high-TOC soil varied between 0 and 60% at the doses $<5\%$. $F_{reduced}$ was highest (23–100%) at the highest biochar dose (5%), but there were significant differences in the performance of the activated biochars (see below).

It was not possible to derive PFAS sorption isotherms as the basis for the K_F-value calculation because of variable leaching (thus, sorption) at lower doses (0.1–1%) for the high-TOC soil and almost complete ($>99\%$) sorption at higher doses (1–5%) for the low-TOC soil. A clear trend of decreasing aqueous concentrations over a certain concentration range with increasing sorbent amount is needed to construct a sorption isotherm (Schwarzenbach et al., 2003). Therefore, mean K_F values for the five doses of each sorbent were calculated by interpolating PFBS, PFHxS, PFOS, and PFBA sorption at the various dosages to leachate water concentrations of 1 ng L^{-1} (assuming nF = 0.7) and interpolating PFHxS and PFOS to concentrations of 1 µg L^{-1} (Table 3, see S.1.2 for details on calculation).

The K_F-values for the biochar sorbents in the low-TOC soil were all equal to or higher than those in the high-TOC soil, with log K_F values ranging from for example, 4.4–6.3 and 3.4–4.4 for PFBS and 4.6–6.4 and 3.0–4.8 for PFOA, for low-TOC and high-TOC soil, respectively. The lower sorbent effectiveness in high-TOC soil can be explained by the presence of high concentrations of organic matter, which attenuate the effect of the biochar sorbent by pore clogging and competitive sorption to pore walls (Cornelissen and Gustafsson, 2006; Kwon and Pignatello, 2005). This attenuation effect has also been demonstrated specifically for PFAS sorption to AC (Du et al., 2014). In addition, the high-TOC soil itself sorbed PFAS about 100-times stronger than the low-TOC soil, requiring stronger sorbents to overcome the sorption of the soil itself and reduce leaching. This OM-related combination of higher intrinsic PFAS-sorption when unamended and an attenuation

Table 2
Concentrations of selected PFAS in study soil (C_{soil}, µg kg^{-1}), leachate (C_w, µg L^{-1}), the portion of a soil PFAS that was leachable ($F_{leachable}$, %, see S.1.2), and the partitioning coefficients between water and soil (logK_D, L kg^{-1}) and water and soil organic carbon (logK_{OC}, L kg^{-1}).

PFAS	CF-chain length	High-TOC					Low-TOC				
		C_{soil} (µg kg^{-1})	C_w (µg L^{-1})	$F_{leachable}$ (%)	logK_D (L kg^{-1})	logK_{OC} (L kg^{-1})	C_{soil} (µg kg^{-1})	C_w (µg L^{-1})	$F_{leachable}$ (%)	logK_D (L kg^{-1})	logK_{OC} (L kg^{-1})
PFBS	4	3.9 ± 0.7	0.084 ± 0.007	22	1.6	2.2	26 ± 2	2.8 ± 0.2	108[a]	[b]	[b]
PFHxS	6	110 ± 24	1.2 ± 0.3	10.9	1.9	2.6	200 ± 18	26 ± 5	130[a]	[b]	[b]
PFOS	8	1000 ± 60	2.9 ± 0.6	2.9	2.5	3.2	3400 ± 200	240 ± 50	71	0.6	2.6
PFBA	3	2.4 ± 0.4	0.096 ± 0.012	40	1.2	1.9	7.7 ± 0.3	1.0 ± 0.1	130[a]	[b]	[b]
PFHxA	5	8.2 ± 1.7	0.32 ± 0.03	39	1.2	1.9	44 ± 3	7.7 ± 0.8	175[a]	[b]	[b]
PFOA	7	6.4 ± 1.1	0.08 ± 0.01	13	1.8	2.5	27 ± 2	2.5 ± 0.3	93	−0.1	1.9
PFAS$_{tot}$	–	1200 ± 80	5.1 ± 0.8	4.3	–	–	3800 ± 240	290 ± 45	76	–	–

− = not applicable.
[a] Amount in leachate exceeded amount in soil due to analytical uncertainty.
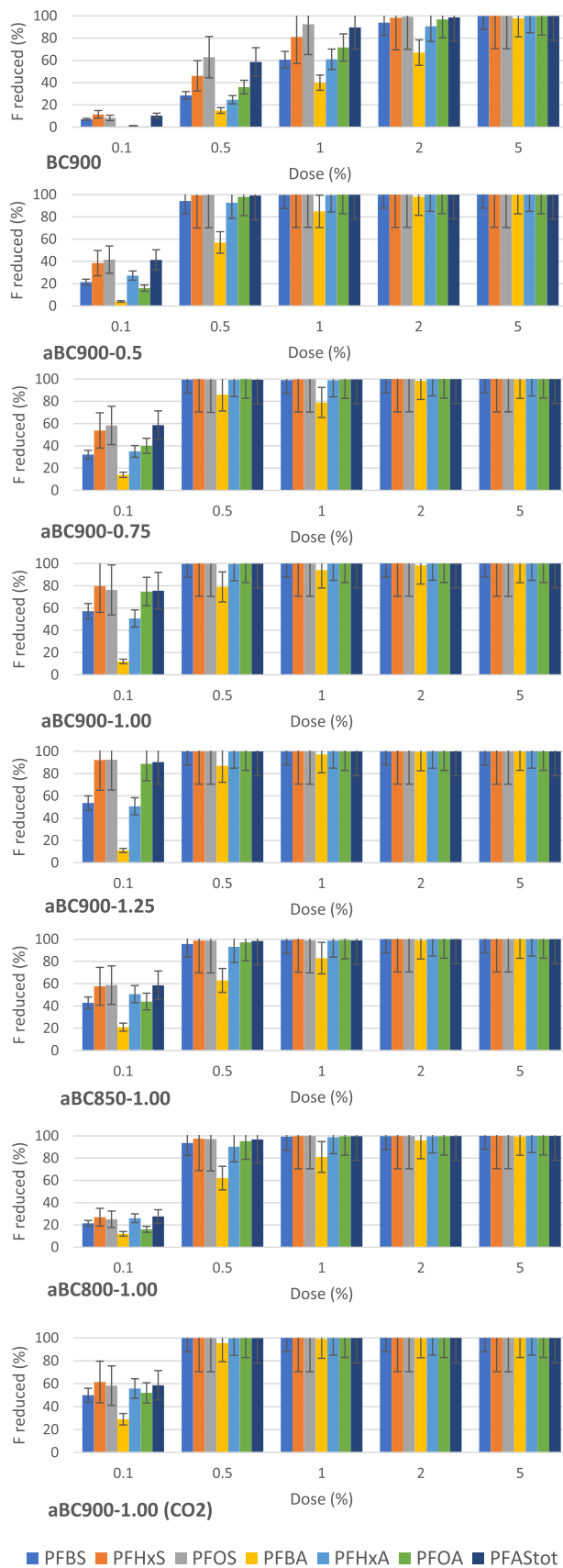[b] No measurable sorption.
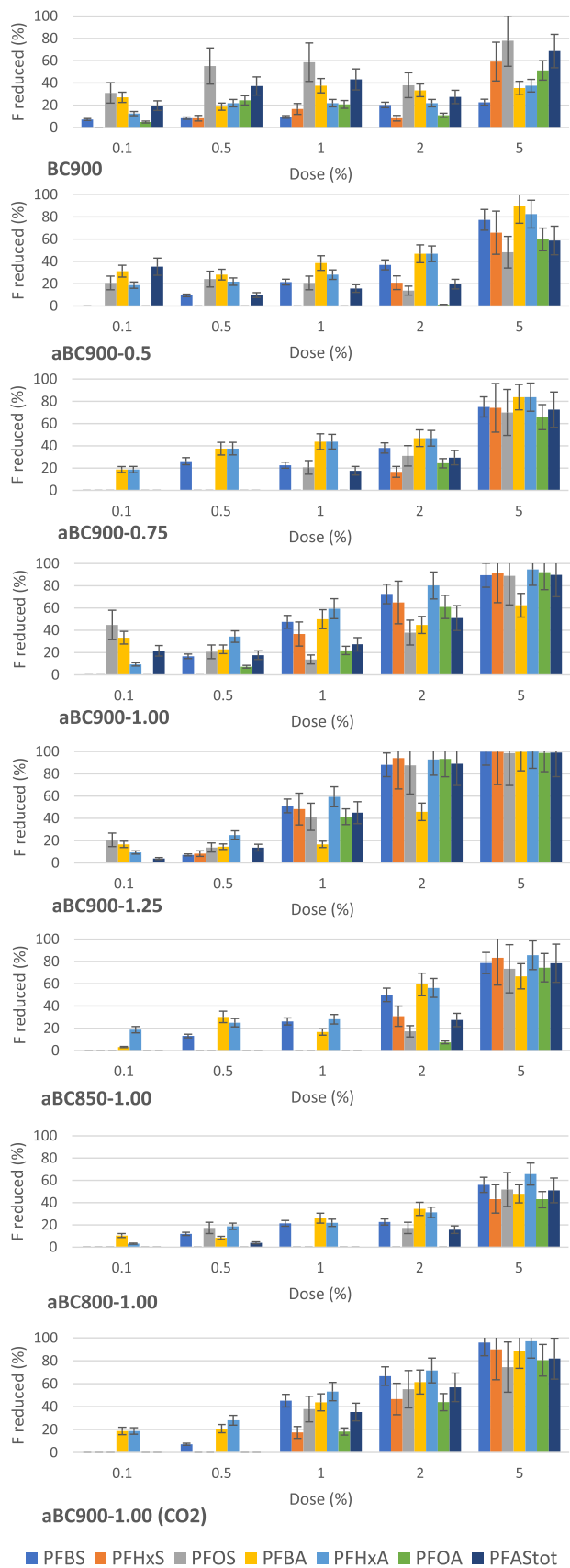
Fig. 1. Reduction in leaching ($F_{reduced}$, %) of PFBS, PFHxS, PFOS, PFBA, PFHxA, PFOA and $PFAS_{tot}$ from high-TOC and low-TOC soil due to addition of different doses (%) of pristine and activated biochar. See text for biochar naming system.

Table 3
Partitioning coefficients (K_F) for PFAS between water and biochar sorbents in the presence of soil, normalized to water concentrations of 1 µg L^{-1} for PFHxS and PFOS and 1 ngL^{-1} for PFBS, PFBA, PFHxA and PFOA. Shown as mean ± standard deviation of K_F-values calculated for 5 different doses of sorbents ($n = 5$). Mean values for which $n < 5$ indicated by: ′ $n = 4$, * $n = 3$, # $n = 2$, + $n = 1$.

Soil	PFAS	Unit	BC900	aBC900-0.5	aBC900-0.75	aBC900-1.00	aBC900-1.25	aBC900-1.00-CO₂	aBC850-1.00	aBC800-1.00
High-TOC	PFHxS	LogK$_{F,sorbent}$	3.1 ± 0.3′	3.3 ± 0.3#	3.3 ± 0.4#	3.8 ± 0.2*	4.2 ± 0.8′	3.6 ± 0.3*	3.5 ± 0.3#	3.1+
	PFOS	(µg kg^{-1})/(µg L^{-1})^n = log K$_{D,sorbent}$ at 1 µg L^{-1}	4.7 ± 0.5	4.2 ± 0.6	4.1 ± 0.1*	4.5 ± 0.6	4.8 ± 0.5	4.3 ± 0.1*	4.0 ± 0.4#	4.0 ± 0.3*
	PFBS	LogK$_{F,sorbent}$	3.4 ± 0.4	3.7 ± 0.1′	3.8 ± 0.2′	4.1 ± 0.2′	4.4 ± 0.9′	4.0 ± 0.4′	3.8 ± 0.1′	3.6 ± 0.2′
	PFBA	(ng kg^{-1})/(ng L^{-1})^n = log K$_{D,sorbent}$ at 1 ng L^{-1}	3.6 ± 0.6	3.9 ± 0.4	3.8 ± 0.3	3.8 ± 0.5	3.9 ± 0.7	3.9 ± 0.3	3.6 ± 0.2	3.4 ± 0.4
	PFHxA		3.6 ± 0.5	3.9 ± 0.3	4.1 ± 0.3	4.2 ± 0.1	4.5 ± 0.7	4.2 ± 0.2	4.0 ± 0.3	3.6 ± 0.1
	PFOA		3.8 ± 0.4	3.0 ± 1.1#	3.8 ± 0.2#	4.1 ± 0.4′	4.8 ± 0.5*	4.0 ± 2.10*	3.6 ± 0.7#	3.6+
Low-TOC	PFHxS	LogK$_{F,sorbent}$	4.0 ± 0.7′	5.0 ± 0.8	5.5 ± 1.1	5.7 ± 0.7	5.8 ± 0.7	5.4 ± 0.7	5.4 ± 1.0	4.6 ± 0.9
	PFOS	(µg kg^{-1})/(µg L^{-1})^n = log K$_{D,sorbent}$ at 1 µg L^{-1}	4.6 ± 0.6	5.5 ± 0.6	5.8 ± 0.9	5.9 ± 0.5	6.0 ± 0.6	5.7 ± 0.6	5.8 ± 0.9	5.2 ± 0.6
	PFBS	LogK$_{F,sorbent}$	4.4 ± 0.7′	5.6 ± 0.9	6.0 ± 1.2	6.1 ± 0.6	6.3 ± 0.8	6.2 ± 0.7	5.7 ± 0.8	5.3 ± 0.7
	PFBA	(ng kg^{-1})/(ng L^{-1})^n = log K$_{D,sorbent}$ at 1 ng L^{-1}	3.7 ± 0.5*	4.4 ± 0.4′	4.9 ± 0.8′	4.7 ± 0.3′	5.0 ± 0.3′	4.9 ± 0.6	4.6 ± 0.5′	4.3 ± 0.3′
	PFHxA		4.4 ± 0.8*	5.6 ± 0.6′	6.3 ± 1.1′	5.9 ± 1.0	6.3 ± 1.2	6.0 ± 0.9	5.6 ± 1.1	5.4 ± 0.6′
	PFOA		4.6 ± 0.6′	5.5 ± 0.8	6.2 ± 1.2	6.4 ± 0.6	6.4 ± 0.8	6.0 ± 0.7	5.8 ± 0.7	5.3 ± 0.6

of sorption effect when amended with biochar, was also observed by Askeland et al. (2020) when comparing the effect of biochar in two different soil types, a loamy sand (9.6% TOC) and a sandy clay loam (1.5% TOC).

Dissolved organic carbon (DOC) in leachates from the low-TOC soil decreased with increasing activated biochar dose (Table S9), demonstrating that the activated biochars possessed sufficient sorption capacity to retain both PFAS and DOC in this soil type. In the high-TOC soil systems, however, DOC leaching was high ($C_W > 300$ mg L^{-1}) and there was no trend between DOC in leachates and activated biochar dose. This indicated sorption site saturation, and this would also apply to PFAS. Higher doses of activated biochar sorbents would thus be necessary to achieve the same relative remediation effect in soils with a high TOC content compared to soils with a low TOC content.

Using the same WT feedstock to produce biochar, although with a simpler, lower-temperature pyrolysis method (Kon-Tiki flame curtain kiln (Cornelissen et al., 2016), 500–650 °C), Silvani et al. (2019) measured biochar logK$_F$-values of 3.38 L kg^{-1} for PFOS and 2.08 L kg^{-1} for PFOA in the same low-TOC soil as used in this study. In comparison, the high temperature (900 °C) biochar produced in this study (BC900) gave K$_F$-values for PFOS and PFOA that were >1.00 log unit higher. Furthermore, the biochars activated at 900 °C (aBC900-0.5-1.25) exhibited K$_F$-values equal to or higher than logK$_F$-values of a commercially produced activated biochar made from coconut shell, 5.00–5.49 L kg^{-1} for PFOS and 4.74–5.42 L kg^{-1} for PFOA, for the same soils that were used in this study (Silvani et al., 2019).

The K$_F$-values for aBC900–0.5-1.25 were all in the same range as logK$_F$-values from commercially-produced activated carbons tested in two other studies: >5.60 L kg^{-1} for PFOS and >5.60 L kg^{-1} for PFOA (Kupryianchyk et al., 2016b), and 5.86 L kg^{-1} for PFOS and 4.45 L kg^{-1} for PFOA (Hansen et al., 2010). This demonstrates the potential of using activated biochars made from a woody waste feedstock to replace activated carbons made from lignite or activated biochars made from high value feedstocks for environmental remediation projects.

3.4.2. Effect of PFAS chain length and functional group

No significant linear correlations ($R^2 < 0.20$, $p > 0.05$, Table S10) between F$_{reduced}$ and CF-chain length were found for any of the eight sorbents when data from both soils were combined (all detected PFSA and PFCA included, CF3–CF10). However, by separating data from the high-TOC and low-TOC soil, two opposing trends were detected.

It is difficult to observe trends in sorption behavior because of the very high PFAS sorption by low-TOC soil with higher biochar doses and very low or variable PFAS sorption by the high-TOC soil with lower biochar doses. Thus, here and in the following subsections, only the low-TOC soil 0.1% dose and the high-TOC soil 5% dose data were

further scrutinized. There was a significant positive linear correlation ($R^2 = 0.42–0.76$, $p < 0.05$) between F$_{reduced}$ and CF-chain length for all the activated biochar sorbents (0.1% dose) in the low-TOC soil (Table S10, Fig. S3). This suggests the importance of hydrophobicity in the adsorption of PFAS to ACs.

Du et al., 2014 summarized that electrostatic interactions are important for the binding of highly electronegative PFAS to various sorbent surfaces, but that the repulsive effect between a negatively charged surface and a PFAS molecule can be overcome by the strong beneficial van der Waals hydrophobic interactions between the CF-chain and e.g. an activated biochar surface. An increased sorption to AC with increasing CF-chain length was also attributed to hydrophobic interactions by Chen et al. (2017) in a batch sorption test with different ACs, and by Sorengard et al. (2019) for colloidal AC in the presence of ten different soil types. In a later batch sorption experiment with 44 different sorbents (including some ACs), however, the same group (Sörengård et al., 2020) found that the correlation between CF-chain length and sorption was not significant for PFCA with short chain lengths (CF3–CF7). They used a principal component analysis to show that electrostatic interactions and hydrophobic interaction mechanisms dominated for short chain and longer chain PFAS adsorption, respectively.

Most biochar surfaces are negatively charged (Ahmad et al., 2014), and this is probably also the case for the activated biochars amended to the low-TOC soil (leachate pH of 7–8, Table S3). Considering the fact that PFSA have been observed to be strong acids and that the pKa-values of PFBA, PFHxA and POFA are 0.394, 0.840 and 0–3.80, respectively (Ding and Peijnenburg, 2013), the PFAS investigated here will have a negative charge given the leachate pH of 7–8 (Table S3). Thus, they all experience electrostatic repulsion from biochar surfaces, which may have had a stronger effect on the short chain PFAS, such as PFBA (CF3) and PFBS (CF4), that have more limited hydrophobic interactions compared to their longer chain counterparts, resulting in the lowest K$_F$-values for these two compounds (Table 3).

There are also indications that the functional head groups affect the degree of adsorption in the currently investigated biochars. F$_{reduced}$ was significantly higher (Welch *t*-test, $p < 0.05$) for PFBS compared to PFPeA (both CF4) for 6 of the 8 biochars in the low-TOC soil (0.1%). For PFSA and PFCA pairs with longer CF-chains there were no significant differences in adsorption. This is in agreement with Sörengård et al. (2020) who showed that PFSA sorb more strongly to a range of sorbents than their PFCA counterparts, and Askeland et al. (2020) who found that PFHxS (CF6) sorbed more strongly to biochar than PFOA (CF7) in the presence of soil. It is speculated that this relation likely is due to PFSA being more hydrophobic than PFCA (de Voogt et al., 2012).

In the high-TOC soil, the opposite trend was observed compared to the low-TOC soil: significant negative linear correlations ($R^2 = 0.52–0.74$, $p < 0.05$, Table S10, Fig. S4) between F$_{reduced}$ and CF-chain

length were observed for five of the eight biochar sorbents (5% dose). Sorengard et al. (2019) observed a decreasing sorption of PFPeA, PFHxA, PFHpA, PFOA and PFBS to colloidal AC with increasing soil OM content in soils and attributed it to steric hindrance, i.e. blocking of the AC pores systems by OM. Since increasing adsorption rates of PFAS to AC with decreasing CF-chain length has been explained by smaller PFAS experiencing less steric effects (Du et al., 2014), it is speculated that short chain PFAS like PFBA and PFBS were less affected by pore blockage, and thus adsorbed by biochars to a greater degree in the high-TOC soil compared to longer CF-chain length PFAS.

3.4.3. Effect of degree of activation

A strong positive linear correlation ($R^2 > 0.9$, $p < 0.05$) between degree of activation and $F_{reduced}$ was found for PFBS, PFHxS, PFHxA and PFOA in the low-TOC (0.1% dose) and high-TOC (5% dose) soils (Fig. 2). This correlation was also significant for PFOS in the low-TOC soil ($R^2 = 0.9998$, $p < 0.05$), but not in the high-TOC soil ($R^2 = 0.2985$, $p > 0.05$). Furthermore, $F_{reduced}$ was significantly higher (Welch t-test, $p < 0.05$) for a highly activated biochar (aBC900-1.25) compared to the non-activated biochar (BC900) for PFBS, PFHxS, PFOS, PFBA, PFHxA and PFOA at the 0.1% dose in low-TOC soil and for PFBS, PFBA, PFHxA and PFOA at the 5% dose in high-TOC soil.

These results show that activation of WT biochar can improve PFAS retention when added to PFAS-contaminated soils of both with high and low TOC contents. Furthermore, considering that there was no significant difference (Wilcoxon test, $p > 0.05$) between the K_F of BC900 and aBC-900-0.50, and aBC900-1.00 and aBC900.1.25, a biochar activated at a molar ratio of oxidant to feedstock C of 0.75–1.00 might be the most effective in terms of PFAS sorption characteristics. It should

be noted however, that increasing the degree of activation comes at a trade off with biochar yield (Table 1).

The observed improvement of sorbent performance with increasing degree of activation was expected when considering the increase in SSA of the larger pores (>1.5 nm) with increasing degree of activation (Table 1), as sorption of organic contaminants to biochar has been positively correlated to SSA (Ahmad et al., 2014; Beesley et al., 2011; Hale et al., 2016). It is possible that the larger pores are more important for sorption of the larger PFAS (CF6 to CF8) as they offer less steric hindrance for molecules with long CF-chains. The molecular lengths of PFOS and PFOA, 1.32 and 1.20 nm respectively (Chen et al., 2017), are indeed close to the upper diameter of the small pores quantified through CO_2 gas absorption (0.3–1.5 nm). This is corroborated by Deng et al. (2015) who found that chemically activated (KOH) biochar made from bamboo adsorbed larger amounts of PFOS and PFOA than what had been reported for granular and powdered ACs, and attributed this effect to enlarged pore systems created through activation.

Another explanation for the observed relation between degree of activation and sorbent performance is that the activation process changes surface chemistry through the creation/destruction of surface functional groups (Hagemann et al., 2018) in a way that is beneficial to hydrophobic or electrostatic interactions with PFAS. Although there was no significant increase/decrease of C/O ratio with degree of activation ($R^2 = 0.004$, $p > > 0.05$), the nature and abundance of O-containing surface functional groups could have been altered by activation. However, analyses of biochar surface chemistry e.g. by X-ray photoelectron spectroscopy or other techniques (cf. Hagemann et al. (2017)) was beyond the scope of this study.
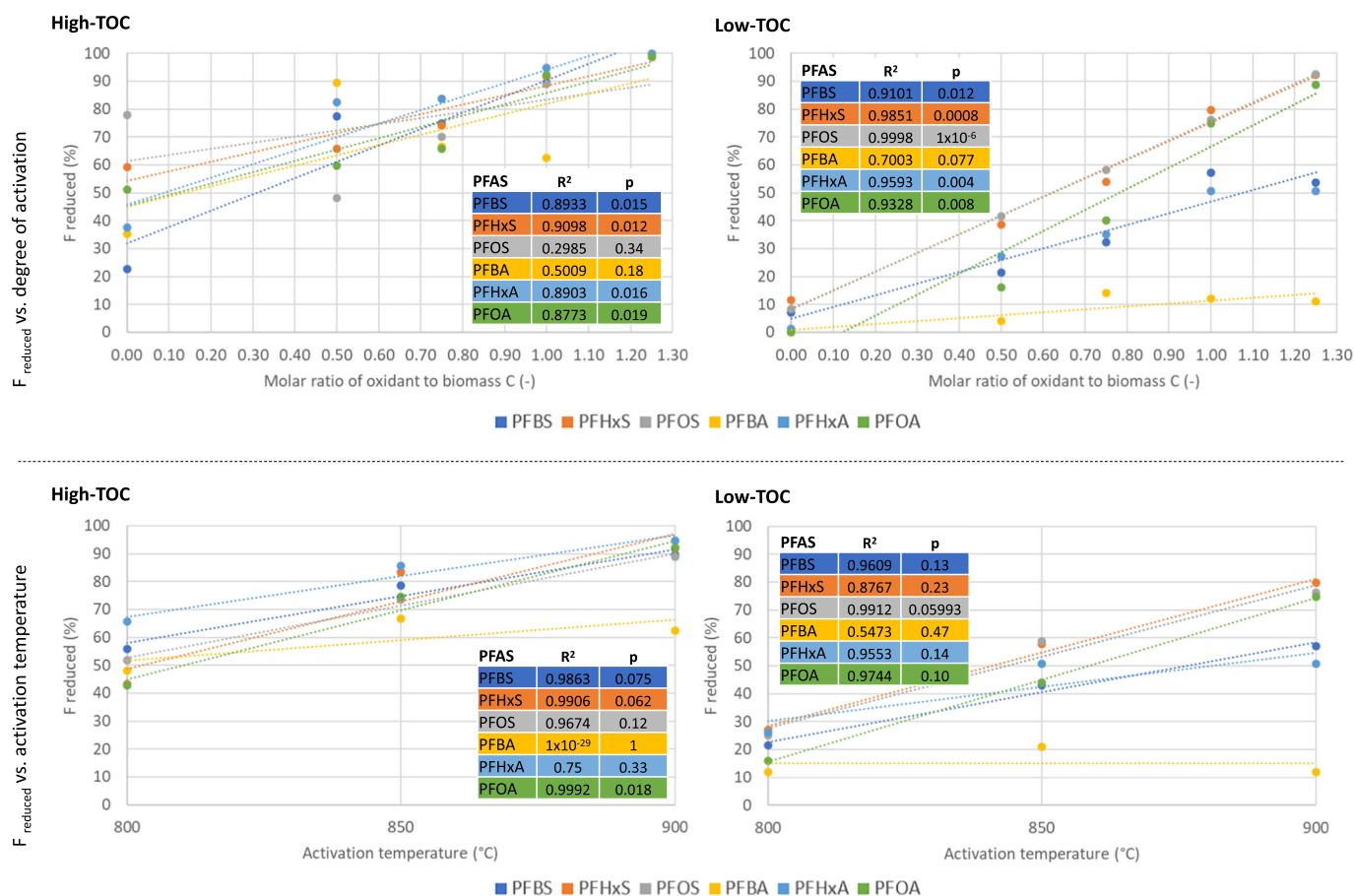

Fig. 2. Reduction in PFAS-leaching from high-TOC and low-TOC soil as a function of molar ratio of oxidant (H_2O) to feedstock C and activation temperature (using a molar ratio of H_2O oxidant to feedstock C of 1.00), plotted for the amendment doses of 5% for high-TOC soil and 0.1% for low-TOC soil.

3.4.4. Effect of activation temperature

Positive correlations ($R^2 > 0.75$) between activation temperature and $F_{reduced}$ were observed in both soils for PFBS, PFHxS, PFOS, PFHxA and PFOA (Fig. 2), but with the exception of PFOA in low-TOC soil, none of the correlations were statistically significant ($p > 0.05$). $F_{reduced}$ was, however, significantly higher (Welch t-test, $p < 0.05$) for aBC900-1.00 than aBC800-1.00 for PFBS, PFHxS, PFOS, PFHxA and PFOA in the low-TOC soil (0.1% dose) and for PFBS and PFOA in the high-TOC soil (5% dose).

The larger large pore (>1.5 nm) SSA of aBC900-1.00 (713 m^2/g) compared to aBC800-1.00 (444 m^2/g), also suggests that the biochar sorbent activated at the highest temperature (900 °C) represented a sorbent with a higher potential for reducing PFAS leaching from soil than the one activated at the lowest temperature (800 °C). As with increasing degree of activation, however, increasing activation temperature comes at a trade off with biochar yield (Table 1).

3.4.5. Effect of activation agent

The use of CO_2 resulted in an activated biochar (aBC900-1.00-CO_2) with a similar remediation efficacy as the one produced with steam activation (aBC900-1.00) (both biochars were activated at 900 °C with a molar ratio of feedstock C to oxidant of 1.00). There were no significant differences (Welch t-test, p > 0.05) between $F_{reduced}$ of the two sorbents (aBC900-1.00 versus aBC900-1.00-CO_2) at any of the doses in the low-TOC soil for PFBS, PFHxS, PFOS, PFHxA and PFOA (Table S3). Similarly, in the high-TOC soil, there were also no significant differences (Welch t-test, p > 0.05) between $F_{reduced}$ of the two sorbents for PFBS, PFHxS, PFOS, PFBA, PFHxA or PFOA at the 2 or 5% doses (Table S4). Some differences were observed at lower doses (0.1–1%), but without any apparent trends. There were also no statistically significant differences (Wilcoxon test, p > 0.05) between the K_F of these two sorbents (aBC900-1.00 versus aBC900-1.00-CO_2, Table 3) for PFBS, PFHxS, PFOS, PFBA, PFHxA or PFOA.

As discussed above, steam and CO_2 activation gave modest differences in pore size distributions (Table 1). With the possible exception of PFBA in high-TOC soil, these differences were not significant enough to have an effect on sorbent performance. It has been shown that activation with CO_2 results in a narrower pore size distribution compared to steam activation (Molina-Sabio et al., 1996), something which potentially could affect PFAS sorbent performance through steric effects, but no study has yet demonstrated such a connection.

4. Conclusion and further considerations

This study has shown that biochar made from WT can be used to reduce the leaching of PFAS from contaminated soil (Fig. 1) and that the effect is improved by using activated biochar, optimally produced at 900 °C with a molar ratio of oxidant to feedstock C between 0.75 and 1.00 with either a steam or CO_2 activation agent (Fig. 2). Furthermore, it has been demonstrated that site-specific soil properties affect sorbent performance because: 1) sorption was significantly weaker in high-TOC soil compared to low TOC-soil (Table 3), 2) weaker sorption was observed for short chain PFAS (CF3–CF4) compared to longer chain PFAS (>CF5) (Table S10), and 3) sorption of PFSA (sulfonates) was stronger than that of PFCA (carboxylic acids). This suggests that soil remediation designs should be tailored to site-specific requirements. For example, higher biochar doses (5% or greater) and/or degree of activation (0.75 oxidant to feedstock C or greater) might be necessary to achieve sufficient reduction in leaching from soils with higher TOC-contents or with a large amount of short chain PFAS.

Potential trade-offs between using activated biochar produced with lower yields and higher energy requirements and using higher doses of non-activated biochar should be considered in a life cycle perspective to assess the most environmentally sustainable option for a specific remediation operation. This assessment should also consider the carbon sequestration by biochar, i.e. carbon dioxide removal or pyrogenic

carbon capture and storage (PyCCS, Schmidt et al. (2019)). For example, in low-TOC soil, strong PFAS stabilization ($F_{reduced} > 90\%$) was observed at low doses (0.1–0.5%) for both non-activated and activated biochar sorbents. In this case activation may not be necessary and higher PyCCS could be achieved by using non-activated biochar produced with higher biochar and carbon yield than the activated biochar. In high-TOC soil on the other hand, the non-activated biochar provided an unsatisfactory reduction in leaching (23–78%) compared to a fully activated biochar (63–95%). In this setting the activated biochars offer the advantage of expanded pore systems that are less prone to clogging.

As the suitability of WT activated biochars as sorbents for soil PFAS has been found equal to commercial alternatives made from fossil or higher value biomass feedstocks, future attention should be directed towards other organic waste fractions as potential biochar sorbent feedstocks. Examples include, garden waste, reject and digestate from biogas production, biological waste from fish farms and abattoirs, as well as sewage sludge. This could prove an environmentally sustainable way to deal with the widespread problem of PFAS leaching from contaminated soils or landfill sites, while simultaneously re-using and valorising waste materials and sequestering carbon – all contributing to a more circular economy.

CRediT authorship contribution statement

Erlend Sørmo: Conceptualization, Methodology, Investigation, Formal analysis, Writing – original draft, Writing – review & editing. **Ludovica Silvani:** Conceptualization, Methodology, Investigation, Writing – review & editing. **Nora Bjerkli:** Investigation, Formal analysis. **Nikolas Hageman:** Conceptualization, Methodology, Investigation, Writing – review & editing. **Andrew R. Zimmerman:** Investigation, Writing – review & editing. **Sarah E. Hale:** Supervision, Funding acquisition, Writing – review & editing. **Caroline Berge Hansen:** Investigation. **Thomas Hartnik:** Supervision, Funding acquisition. **Gerard Cornelissen:** Supervision, Funding acquisition, Conceptualization, Methodology, Formal analysis, Writing – review & editing.

Declaration of competing interest

The authors declare that they have no known competing financial interests or personal relationships that could have appeared to influence the work reported in this paper.

Acknowledgements

Appendix A. Supplementary data

Supplementary data to this article can be found online at https://doi.org/10.1016/j.scitotenv.2020.144034.

References

Agrafioti, E., Bouras, G., Kalderis, D., Diamadopoulos, E., 2013. Biochar production by sewage sludge pyrolysis. J. Anal. Appl. Pyrolysis 101, 72–78.

Ahmad, M., Rajapaksha, A.U., Lim, J.E., Zhang, M., Bolan, N., Mohan, D., et al., 2014. Biochar as a sorbent for contaminant management in soil and water: a review. Chemosphere 99, 19–33.

Alhashimi, H.A., Aktas, C.B., 2017. Life cycle environmental and economic performance of biochar compared with activated carbon: a meta-analysis. Resour. Conserv. Recycl. 118, 13–26.

AMAP, 2016. In: Carlsson, P., Christensen, J.H., Borgå, K., Kallenborn, R., Pfaffhuber, K.A., Odland, J.Ø., et al. (Eds.), Influence of Climate Change on Transport, Levels, and Effects of Contaminants in Northern Areas – Part 2. Arctic Monitoring and Assessment Programme (AMAP), Oslo, p. 52.

Askeland, M., Clarke, B., Paz-Ferreiro, J., 2019. Comparative characterization of biochars produced at three selected pyrolysis temperatures from common woody and herbaceous waste streams. PeerJ 7, e6784.

Askeland, M., Clarke, B.O., Cheema, S.A., Mendez, A., Gasco, G., Paz-Ferreiro, J., 2020. Biochar sorption of PFOS, PFOA, PFHxS and PFHxA in two soils with contrasting texture. Chemosphere 249, 126072.

Aworn, A., Thiravetyan, P., Nakbanpote, W., 2008. Preparation and characteristics of agricultural waste activated carbon by physical activation having micro- and mesopores. J. Anal. Appl. Pyrolysis 82, 279–285.

Baharak, S., Wei-Yin, C., Nosa, O.E., 2019. A comprehensive review on physical activation of biochar for energy and environmental applications. Rev. Chem. Eng. 35, 735–776.

Banzhaf, S., Filipovic, M., Lewis, J., Sparrenbom, C.J., Barthel, R., 2017. A review of contamination of surface-, ground-, and drinking water in Sweden by perfluoroalkyl and polyfluoroalkyl substances (PFASs). Ambio 46, 335–346.

Beesley, L., Moreno-Jiménez, E., Gomez-Eyles, J.L., Harris, E., Robinson, B., Sizmur, T., 2011. A review of biochars' potential role in the remediation, revegetation and restoration of contaminated soils. Environ. Pollut. 159, 3269–3282.

Benedetti, V., Patuzzi, F., Baratieri, M., 2017. Gasification char as a potential substitute of activated carbon in adsorption applications. Energy Procedia 105, 712–717.

Bernardo, M., Lapa, N., Gonçalves, M., Mendes, B., Pinto, F., Fonseca, I., et al., 2012. Physicochemical properties of chars obtained in the co-pyrolysis of waste mixtures. J. Hazard. Mater. 219-220, 196–202.

Campos Pereira, H., Ullberg, M., Kleja, D.B., Gustafsson, J.P., Ahrens, L., 2018. Sorption of perfluoroalkyl substances (PFASs) to an organic soil horizon – effect of cation composition and pH. Chemosphere 207, 183–191.

Chen, S.-J., Su, H.-B., Chang, J.-E., Lee, W.-J., Huang, K.-L, Hsieh, L.-T., et al., 2007. Emissions of polycyclic aromatic hydrocarbons (PAHs) from the pyrolysis of scrap tires. Atmos. Environ. 41, 1209–1220.

Chen, S., Jiao, X.-C., Gai, N., Li, X.-J., Wang, X.-C., Lu, G.-H., et al., 2016. Perfluorinated compounds in soil, surface water, and groundwater from rural areas in eastern China. Environ. Pollut. 211, 124–131.

Chen, W., Zhang, X., Mamadiev, M., Wang, Z., 2017. Sorption of perfluorooctane sulfonate and perfluorooctanoate on polyacrylonitrile fiber-derived activated carbon fibers: in comparison with activated carbon. RSC Adv. 7, 927–938.

Chiou, C.T., McGroddy, S.E., Kile, D.E., 1998. Partition characteristics of polycyclic aromatic hydrocarbons on soils and sediments. Environ. Sci. Technol. 32, 264–269.

Clara, M., Scharf, S., Weiss, S., Gans, O., Scheffknecht, C., 2008. Emissions of perfluorinated alkylated substances (PFAS) from point sources—identification of relevant branches. Water Sci. Technol. 58, 59–66.

Cornelissen, G., Gustafsson, Ö., 2006. Effects of added PAHs and precipitated humic acid coatings on phenanthrene sorption to environmental black carbon. Environ. Pollut. 141, 526–531.

Cornelissen, G., Amstaetter, K., Hauge, A., Schaanning, M., Beylich, B., Gunnarsson, J.S., et al., 2012. Large-scale Field study on thin-layer capping of marine PCDD/F-contaminated sediments in Grenlandfjords, Norway: physicochemical effects. Environ. Sci. Technol. 46, 12030–12037.

Cornelissen, et al., 2005. Extensive sorption of organic compounds to black carbon, coal, and kerogen in sediments and soils: Mechanisms and consequences for distribution, bioaccumulation, and biodegradation. Environ. Sci. Technol. 39 (18), 6881–6895. https://doi.org/10.1021/es050191b.

Cornelissen, G., Pandit, N.R., Taylor, P., Pandit, B.H., Sparrevik, M., Schmidt, H.P., 2016. Emissions and char quality of flame-curtain "Kon Tiki" kilns for farmer-scale charcoal/biochar production. PLoS One 11, e0154617.

Deng, S., Nie, Y., Du, Z., Huang, Q., Meng, P., Wang, B., et al., 2015. Enhanced adsorption of perfluorooctane sulfonate and perfluorooctanoate by bamboo-derived granular activated carbon. J. Hazard. Mater. 282, 150–157.

Devi, P., Saroha, A.K., 2014. Risk analysis of pyrolyzed biochar made from paper mill effluent treatment plant sludge for bioavailability and eco-toxicity of heavy metals. Bioresour. Technol. 162, 308–315.

Ding, G., Peijnenburg, W.J.G.M., 2013. Physicochemical properties and aquatic toxicity of poly- and perfluorinated compounds. Crit. Rev. Environ. Sci. Technol. 43, 598–678.

Du, Z., Deng, S., Bei, Y., Huang, Q., Wang, B., Huang, J., et al., 2014. Adsorption behavior and mechanism of perfluorinated compounds on various adsorbents—a review. J. Hazard. Mater. 274, 443–454.

Ehlers, L.J., Luthy, R.G., 2003. Peer reviewed: contaminant bioavailability in soil and sediment. Environ. Sci. Technol. 37, 295A–302A.

Gallen, C., Eaglesham, G., Drage, D., Nguyen, T.H., Mueller, J.F., 2018. A mass estimate of perfluoroalkyl substance (PFAS) release from Australian wastewater treatment plants. Chemosphere 208, 975–983.

Ghosh, U., Luthy, R.G., Cornelissen, G., Werner, D., Menzie, C.A., 2011. In-situ sorbent amendments: a new direction in contaminated sediment management. Environ. Sci. Technol. 45, 1163–1168.

Grycová, B., Koutník, I., Pryszcz, A., 2016. Pyrolysis process for the treatment of food waste. Bioresour. Technol. 218, 1203–1207.

Hagemann, N., Joseph, S., Schmidt, H.-P., Kammann, C.I., Harter, J., Borch, T., et al., 2017. Organic coating on biochar explains its nutrient retention and stimulation of soil fertility. Nat. Commun. 8, 1089.

Hagemann, N., Spokas, K., Schmidt, H.-P., Kägi, R., Böhler, A.M., Bucheli, D.T., 2018. Activated carbon, biochar and charcoal: linkages and synergies across pyrogenic carbon's ABCs. Water 10.

Hagemann, N., Schmidt, H.-P., Kägi, R., Böhler, M., Sigmund, G., Maccagnan, A., et al., 2020. Wood-based activated biochar to eliminate organic micropollutants from biologically treated wastewater. Sci. Total Environ. 138417.

Hale, S.E., Elmquist, M., Brändli, R., Hartnik, T., Jakob, L., Henriksen, T., et al., 2012. Activated carbon amendment to sequester PAHs in contaminated soil: a lysimeter field trial. Chemosphere 87, 177–184.

Hale, S.E., Arp, H.P.H., Kupryianchyk, D., Cornelissen, G., 2016. A synthesis of parameters related to the binding of neutral organic compounds to charcoal. Chemosphere 144, 65–74.

Hale, S.E., Arp, H.P.H., Slinde, G.A., Wade, E.J., Bjørseth, K., Breedveld, G.D., et al., 2017. Sorbent amendment as a remediation strategy to reduce PFAS mobility and leaching in a contaminated sandy soil from a Norwegian firefighting training facility. Chemosphere 171, 9–18.

Hansen, M.C., Børresen, M.H., Schlabach, M., Cornelissen, G., 2010. Sorption of perfluorinated compounds from contaminated water to activated carbon. J. Soils Sediments 10, 179–185.

Hao, W., Björkman, E., Lilliestråle, M., Hedin, N., 2013. Activated carbons prepared from hydrothermally carbonized waste biomass used as adsorbents for CO_2. Appl. Energy 112, 526–532.

Helsen, L., Van den Bulck, E., 2000. Metal behavior during the low-temperature pyrolysis of chromated copper arsenate-treated wood waste. Environ. Sci. Technol. 34, 2931–2938.

Higgins, C.P., Luthy, R.G., 2006. Sorption of perfluorinated surfactants on sediments. Environ. Sci. Technol. 40, 7251–7256.

Jin, H., Zhang, Y., Zhu, L., Martin, J.W., 2015. Isomer profiles of perfluoroalkyl substances in water and soil surrounding a Chinese fluorochemical manufacturing park. Environ. Sci. Technol. 49, 4946–4954.

Keiluweit, M., Nico, P.S., Johnson, M.G., Kleber, M., 2010. Dynamic molecular structure of plant biomass-derived black carbon (biochar). Environ. Sci. Technol. 44, 1247–1253.

Kottek, M., Grieser, J., Beck, C., Rudolph, B., Rubel, F., 2006. World map of the Köppen-Geiger climate classification updated. Meteorol. Z. 15, 259–263.

Krafft, M.P., Riess, J.G., 2015. Per- and polyfluorinated substances (PFASs): environmental challenges. Curr. Opin. Colloid Interface Sci. 20, 192–212.

Kupryianchyk, D., Hale, S., Zimmerman, A.R., Harvey, O., Rutherford, D., Abiven, S., et al., 2016a. Sorption of hydrophobic organic compounds to a diverse suite of carbonaceous materials with emphasis on biochar. Chemosphere 144, 879–887.

Kupryianchyk, D., Hale, S.E., Breedveld, G.D., Cornelissen, G., 2016b. Treatment of sites contaminated with perfluorinated compounds using biochar amendment. Chemosphere 142, 35–40.

Kwon, S., Pignatello, J.J., 2005. Effect of natural organic substances on the surface and adsorptive properties of environmental black carbon (char): pseudo pore blockage by model lipid components and its implications for N2-probed surface properties of natural sorbents. Environ. Sci. Technol. 39, 7932–7939.

Lang, J.R., Allred, B.M., Field, J.A., Levis, J.W., Barlaz, M.A., 2017. National estimate of per- and polyfluoroalkyl substance (PFAS) release to U.S. Municipal Landfill Leachate. Environ. Sci. Technol. 51, 2197–2205.

Lau, C., Anitole, K., Hodes, C., Lai, D., Pfahles-Hutchens, A., Seed, J., 2007. Perfluoroalkyl acids: a review of monitoring and toxicological findings. Toxicol. Sci. 99, 366–394.

Lehmann, J., Joseph, S., 2015. Biochar for Environmental Management: Science, Technology and Implementation. Routledge.

Mahinroosta, R., Senevirathna, L., 2020. A review of the emerging treatment technologies for PFAS contaminated soils. J. Environ. Manag. 255, 109896.

Marsh, H., Reinoso, F.R., 2006. Activated Carbon. Elsevier Science.

Martin, M.J., Balaguer, M.D., Rigola, M., 1996. Feasibility of activated carbon production from biological sludge by chemical activation with ZnCl2 and H2SO4. Environ. Technol. 17, 667–671.

Molina-Sabio, M., Gonzalez, M.T., Rodriguez-Reinoso, F., Sepúlveda-Escribano, A., 1996. Effect of steam and carbon dioxide activation in the micropore size distribution of activated carbon. Carbon 34, 505–509.

NGUa. Løsmasser. Nasjonal løsmassedatabase. Norwegian Geological Survey (NGU), Norway, (pp. Digital quarternary geology database and map for Norway).

NGUb. Berggrunn. Nasjonal berggrunnsdatabase. Norwegian Geological Survey (NGU), Norway, (pp. Digital bedrock database and map for Norway).

Rajapaksha, A.U., Chen, S.S., Tsang, D.C.W., Zhang, M., Vithanage, M., Mandal, S., et al., 2016. Engineered/designer biochar for contaminant removal/immobilization from soil and water: potential and implication of biochar modification. Chemosphere 148, 276–291.

Rankin, K., Mabury, S.A., Jenkins, T.M., Washington, J.W., 2016. A North American and global survey of perfluoroalkyl substances in surface soils: distribution patterns and mode of occurrence. Chemosphere 161, 333–341.

Schmidt, H.-P., Anca-Couce, A., Hagemann, N., Werner, C., Gerten, D., Lucht, W., et al., 2019. Pyrogenic carbon capture and storage. GCB Bioenergy 11, 573–591.

Schwarzenbach, R.P., Geschwend, P.M., Imboden, D.M., 2003. Environmental Organic Chemistry. John Wiley & Sons, Inc, Hoboken, New Jersey.

Sepulvado, J.G., Blaine, A.C., Hundal, L.S., Higgins, C.P., 2011. Occurrence and fate of perfluorochemicals in soil following the land application of municipal biosolids. Environ. Sci. Technol. 45, 8106–8112.

Silvani, L., Cornelissen, G., Botnen Smebye, A., Zhang, Y., Okkenhaug, G., Zimmerman, A.R., et al., 2019. Can biochar and designer biochar be used to remediate per- and polyfluorinated alkyl substances (PFAS) and lead and antimony contaminated soils? Sci. Total Environ. 694, 133693.

Skaar, J.S., Ræder, E.M., Lyche, J.L., Ahrens, L., Kallenborn, R., 2019. Elucidation of contamination sources for poly- and perfluoroalkyl substances (PFASs) on Svalbard (Norwegian Arctic). Environ. Sci. Pollut. Res. 26, 7356–7363.

Sorengard, M., Kleja, D.B., Ahrens, L., 2019. Stabilization of per- and polyfluoroalkyl substances (PFASs) with colloidal activated carbon (PlumeStop®) as a function of soil clay and organic matter content. J. Environ. Manag. 249, 109345.

Sörengård, M., Kleja, D.B., Ahrens, L., 2019. Stabilization and solidification remediation of soil contaminated with poly- and perfluoroalkyl substances (PFASs). J. Hazard. Mater. 367, 639–646.

Sörengård, M., Östblom, E., Köhler, S., Ahrens, L., 2020. Adsorption behavior of per- and polyfluoralkyl substances (PFASs) to 44 inorganic and organic sorbents and use of dyes as proxies for PFAS sorption. J. Environ. Chem. Eng. 8, 103744.

Sørmo, E., Silvani, L., Thune, G., Gerber, H., Schmidt, H.P., Smebye, A.B., et al., 2020. Waste timber pyrolysis in a medium-scale unit: Emission budgets and biochar quality. Sci. Total Environ. 718, 137335.

Sparrevik, M., Saloranta, T., Cornelissen, G., Eek, E., Fet, A.M., Breedveld, G.D., et al., 2011. Use of life cycle assessments to evaluate the environmental footprint of contaminated sediment remediation. Environ. Sci. Technol. 45, 4235–4241.

SSB, 2018. Waste Accounts 2012–2018. 2020. Statistics Norway (SSB).

Sunderland, E.M., Hu, X.C., Dassuncao, C., Tokranov, A.K., Wagner, C.C., Allen, J.G., 2019. A review of the pathways of human exposure to poly- and perfluoroalkyl substances (PFASs) and present understanding of health effects. J. Expo. Sci. Environ. Epidemiol. 29, 131–147.

de Voogt, P., Zurano, L., Serné, P., Haftka, J.J.H., 2012. Experimental hydrophobicity parameters of perfluorinated alkylated substances from reversed-phase high-performance liquid chromatography. Environ. Chem. 9 (6), 564–570.

Zareitalabad, P., Siemens, J., Hamer, M., Amelung, W., 2013. Perfluorooctanoic acid (PFOA) and perfluorooctanesulfonic acid (PFOS) in surface waters, sediments, soils and wastewater – a review on concentrations and distribution coefficients. Chemosphere 91, 725–732.

Zhang, X., Wang, H., He, L., Lu, K., Sarmah, A., Li, J., et al., 2013. Using biochar for remediation of soils contaminated with heavy metals and organic pollutants. Environ. Sci. Pollut. Res. 20, 8472–8483.

Zhao, L., Cao, X., Mašek, O., Zimmerman, A., 2013. Heterogeneity of biochar properties as a function of feedstock sources and production temperatures. J. Hazard. Mater. 256-257, 1–9.

Zhurinsh, A., Zandersons, J., Dobele, G., 2005. Slow pyrolysis studies for utilization of impregnated waste timber materials. J. Anal. Appl. Pyrol. 74, 439–444.